

Supplementary Material

2'FY-RNA aptamers form metastable multimeric G-quadruplexes that selectively bind pyoverdines

Sharif Anisuzzaman, Joshua Alterman, George A Kraus, and Marit Nilsen-Hamilton

Table of contents:

- 1 Synthesis of pyoverdine chromophores
- 2 Aptamer selection
- 3 Supplementary Tables
 - Table S1: Nucleic acid sequences used in this study.
 - Table S2: Conditions of selection in the SELEX protocol
- 4 Supplementary Figures
 - S1: uv/vis absorption spectra of synthesized compounds 1-4
 - S2: Analysis of NextGen sequencing results
 - S3: 2D structures predicted for the aptamers
 - S4: The effect of aptamers on the fluorescence spectrum of HPTA-1
 - S5: The effect of freeze-thaw on the CD spectrum and molecular size of 57PYO3A
 - S6: The effect of salt combinations on PVD-Pf5 binding to 57PYO3A
 - S7-S12: Smoothed overlaid on raw spectra
 - S13: Complete gel images used for manuscript figures
- 5 Citations

Supplementary materials

1 Synthesis of pyoverdine chromophores

Amide ester acid 4. To a round bottom was added nitro lactam A followed by ethyl bromoacetate, DMF, and NaH. The solution was heated to 100°C overnight and quenched with aq. sodium bicarbonate. Washes with ethyl acetate were done 3x (10 mL/ 1 mmol) and the organics were dried over sodium sulfate. The solution was filtered over cotton and concentrated in vacuo. The crude material was separated by column chromatography with ethyl acetate and hexane gave the desired nitro lactam ester plus some O-alkylated product. ¹H NMR (400 MHz, Chloroform-d) δ 8.64 (s, 1H), 7.08 (s, 1H), 6.53 (s, 1H), 5.15 (s, 2H), 4.25 (q, J = 7.1 Hz, 2H), 4.00 (s, 3H), 3.96 (s, 3H), 1.37 – 1.17 (m, 3H). ¹³C NMR (101 MHz, Chloroform-d) δ 167.30, 156.29, 154.06, 146.70, 138.11, 136.14, 110.66, 110.42, 96.53, 96.49, 62.19, 56.49, 56.34, 44.76, 14.19. The nitro group was reduced using excess Fe and aqueous HCl in ethanol. The resulting product was acylated with succinic anhydride to provide amide ester acid 4.

Nitro azetidine ester 1. To an oven dried flask was charged nitro lactam A followed by thionyl chloride (20-30 mol. Eq.) and catalytic amounts of DMF. The solution was heated to 98 °C and left to react overnight. Upon cooling, 2-chloro-6,7-dimethoxy-3-nitro quinoline precipitates as a solid. Thionyl chloride was vacuum distilled at 60 °C with two cold traps until dry. The yellow chloro quinoline obtained was used either in its crude state or re-dissolved in DCM and washed with brine. DCM was dried over sodium sulfate and filtered, and the solvent removed in vacuo to give a yellow solid. ¹H NMR (400 MHz, Chloroform-d) δ 8.63 (s, 1H), 7.41 (s, 1H), 7.14 (s, 1H), 4.07 (s, 3H), 4.05 (s, 3H).

To an oven dried flask was charged 2-chloro-6,7-dimethoxy-3-nitro quinoline and the azetidine ester (1 mol. Eq.), followed by DMF (3mL / 1 mmol) and TEA (2.1 mol. Eq.). The solution was heated to 92 °C and stirred overnight. The DMF was vacuum distilled off and the crude material was dissolved in DCM and wet loaded onto a column. Separation with a gradient of hexane:ethyl acetate (1:0 – 6:4) afforded compound 1 as a red solid (~80% yield). ¹H NMR (400 MHz, Chloroform-d) δ 8.54 (s, 1H), 7.05 (s, 1H), 6.94 (s, 1H), 5.20 (dd, J = 9.5, 5.6 Hz, 1H), 4.42 (td, J = 8.9, 6.3 Hz, 1H), 4.05- 3.98 (m, 1H), 4.01 (s, 3H), 3.96 (s, 3H), 3.73 (s, 3H, O₂Me), 2.71 (dtd, J = 10.7, 9.2, 6.3 Hz, 1H), 2.38 (ddt, J = 11.0, 9.0, 5.7 Hz, 1H). ¹H NMR (400 MHz, DMSO-d6) δ 8.77 (s, 1H), 7.37 (s, 1H), 6.97 (s, 1H), 5.08 (dd, J = 9.7, 5.9 Hz, 1H), 4.17 (q, J = 8.3 Hz, 1H), 3.99-3.81(m, 1H), 3.93 (s, 3H), 3.85 (s, 3H), 3.67 (s, 3H), 2.75 – 2.59 (m, 1H), 2.31 (tt, J = 10.7, 5.7 Hz, 1H). ¹³C NMR (101 MHz, DMSO-d6) δ 172.30, 156.27, 148.78, 148.42, 146.74, 134.46, 131.56, 116.96, 1s07.16, 105.61, 62.03, 56.44, 56.11, 52.41, 50.69, 31.12.

Amino acid 2 and amide acid 3. A flask was charged with 1 followed by hydroiodic acid (~6 mL/ 1 mmol) and allowed to stir until homogenized. The solution was then heated to 66 °C until dry. The beige material was analyzed without purification. ¹H NMR (400 MHz, DMSO-d6) δ 11.37 (s, 1H), 9.03 (s, 1H), 7.52 (s, 2H), 7.30 (s, 1H), 7.09 (s, 1H), 4.40 (d, J = 5.8 Hz, 1H), 3.83 (s, 3H), 3.79 (s, 3H), 3.51 (q, J = 6.1 Hz, 1H), 3.26 (dq, J = 40.4, 8.4 Hz, 2H), 1.92 (q, J = 7.3 Hz, 1H). The crude product was dissolved in chloroform and treated with excess acetic anhydride.

Supplementary materials

2 Aptamer selection

This protocol was designed to isolate aptamers with the characteristics of high affinities and specificities for the ligand and for switching structure on binding the ligand. In addition, the presence of complementary oligonucleotides to the PCR primer sequences during selection limited structure selection to the single-stranded central randomized region. Aptamer selection started with a high molar ratio of pool to PVD-Pf5 (1:1) and a harmonic increase of pool to target PVD-Pf5 in later cycles to increase the selection pressure¹. Counter selections were performed after rounds 3 and 6 against a mixture of two other siderophores, enterobactin (ENB) and ornibactin (ORB), to eliminate nonspecific binders (Fig. 1A). With the assumption that the oligonucleotide complex with PVD-Pf5 is stoichiometric, this selection protocol resulted in 60% of PVD-Pf5 bound by oligonucleotide by round 9 (Fig. 1C). Analysis of the NextGen sequencing results showed that incremental rounds of selection were characterized by increases in the unique fraction (number of sequences in the pool divided by the pool size) and the enriched species (sequences present in the pool more than once), which is characteristic of a successful selection procedure (Fig. S2).

The results of next generation sequencing for oligonucleotide pools from several rounds, including the final round of each selection provided the data for identifying potential aptamer sequences. Sequence clusters were identified with Aptasuite² and, based on the size of the cluster and the rise in enriched species through the rounds, several oligonucleotides were evaluated for binding the PVD-Pf5 chromophore by identifying increases in pyoverdine fluorescence when bound to the oligonucleotide.

Supplementary materials

3 Supplementary tables

Table S1. Nucleic acid sequences used in this study.

Commented [MN1]: Sharif, Please correct/update this table

Name	Sequence
Oligo 5627	TAATACGACTCACTATAAGGGAGACAAGAATAAACGCTC
Oligo 5628	GAGCGTTATTCTTGTCTCCC
Oligo 5629	GCCTGTTGTGAGCCTCTGTCGAA
Oligo 5637	GCCTGTTGTGAGCCTCTGTCGAAGTATGCCATAGGAGCGAATGATATATATCACT TACCAACCGGATGTACTTGTGAGCGTTATTCTTGTCTCCC
Oligo 5651	GGGAGACAAGAAUAAAACGCUCCCCAAAGAGCACCUCAUCCGAUGGUCGUUUUCGC ACAUUCGCUCCGCGAUAGACGUUCGACAGGAGGCUCACAAACAGGC
Oligo 5652	GGGAGACAAGAAUAAAACGCUCCGCUACGAAAGAACUUCUCCGUAACGUGCCAAAU UCAUUCGCUCCGAAUUGGGCAUUCGACAGGAGGCUCACAAACAGGC
Oligo 5653	GGGAGACAAGAAUAAAACGCUCCGCUACUGAUGCUAGAUCUCUCAAUGUGG GCAUUCGCUCCGGGUUGACGUUUCGACAGGAGGCUCACAAACAGGC
Oligo 5654	GGGAGACAAGAAUAAAACGCUCCGACGUUCAGAAAACGAACAGUCUAGUGUCGUCG ACAUUCGCUCCCGGUUGAUGCUUUCGACAGGAGGCUCACAAACAGGC
Oligo 5662	GGGAGACAAGAAUAAAACGCUCCGCUCAUUAACAUUGCUAUUGAGCGCGUCAUAUUG ACAUUCGCUCCCAUUAUGGGCUUCGACAGGAGGCUCACAAACAGGC
Oligo 5663	GGGAGACAAGAAUAAAACGCUCCGCUUGCAUGCAAUAGAACUCCAGCAAGUAGCACAG UCAUUCGCUCCCGUGAUGCUUUCGACAGGAGGCUCACAAACAGGC
Oligo 5664	GGGAGACAAGAAUAAAACGCUCCACACGCCACUCUCAAUGGUGUGACAGCAAUC ACAUUCGCUCCAGAUUGAGGCUUCGACAGGAGGCUCACAAACAGGC
Oligo 5665	GGGAGACAAGAAUAAAACGCUCCGUGGAUGCAUCUGAGUACUACGUAGCGCGUUU ACAUUCGCUCCCAUUGGGCUUCGACAGGAGGCUCACAAACAGGC
Oligo 5666	GGGAGACAAGAAUAAAACGCUCCGAGUCACGAAACAUGCCUCGUCGUACCGCG ACAUUCGCUCCACGUUAUGAGCUUCGACAGGAGGCUCACAAACAGGC
Oligo 5667	GGGAGACAAGAAUAAAACGCUCCACCGUACCGCACACGGCAAGCUAACGAUGUCG ACAUUCGCUCCCGAGCUGAGUUUCGACAGGAGGCUCACAAACAGGC
Oligo 5668	GGGAGACAAGAAUAAAACGCUCCGAGUCACGAAACAUGCCUCGUCGUACCGCG ACAUUCGCUCCCUUGUGAGUAUUCGACAGGAGGCUCACAAACAGGC
Oligo 5669	GGGAGACAAGAAUAAAACGCUCCGUAGGGCUUCGACAGGAGGCUCACAAACAGGC ACAUUCGCUCCCUUGUAGGGCUUCGACAGGAGGCUCACAAACAGGC
58PY01A	GGGCCAAGAGCACUCCAUCGAUGGUCGUUUUCGCACAUUCGCUCCCGGAUAG ACG
57PY03A	GGGACCGUUCAGAAAACGAACAGUCUAGUGUCGUCGACAUUCGCUCCGGUGAUG CU
49BRC1A	GAGACGGUCGGGUCCAGAUUUCGUACUGUCGAGUAGAGUGUGGGUC
15THR1A	GGTTGGTGTGGTTGG
20THR2A	GGTTGGTGTGGTTGGCAACC
32THR4A	GGTAGGGCAGGTTGGGTGTTTCACTTTGGG
97SPN2A	GGGAUGUAACUGAAUGAAAUGGUGAAGGACGGGUCCAGUAGGCUGCUUCGGCAGC CUACUUGUUGAGUAGAGUGUGAGCUCCGUAACUAGUACAUC

Supplementary materials

Table S2. Conditions of selection in the SELEX protocol

Round	2' FY-RNA: PWD-Pf5	Target	Length of capture oligo (nt)	Incubation temperature (°C)
1	1:1	16 μM PVD-Pf5	6	4
2	2:1	5.5 μM PVD-Pf5	6	4
3	3:1	3.5 μM PVD-Pf5	7	4
Counter selection	1:1	10.5 μM ENB and 10.5 μM ORB	7	4
4	5:1	3.5 μM PVD-Pf5	8	4
5	6:1	1 μM PVD-Pf5	8	23
6	7:1	0.6 μM PVD-Pf5	8	23
Counter selection	1:1	3.2 μM ENB and 3.2 μM ORB	8	23
7	8:1	0.4 μM PVD-Pf5	8	23
8	10:1	0.2 μM PVD-Pf5	9	23
9	10:1	0.2 μM PVD-Pf5	9	23

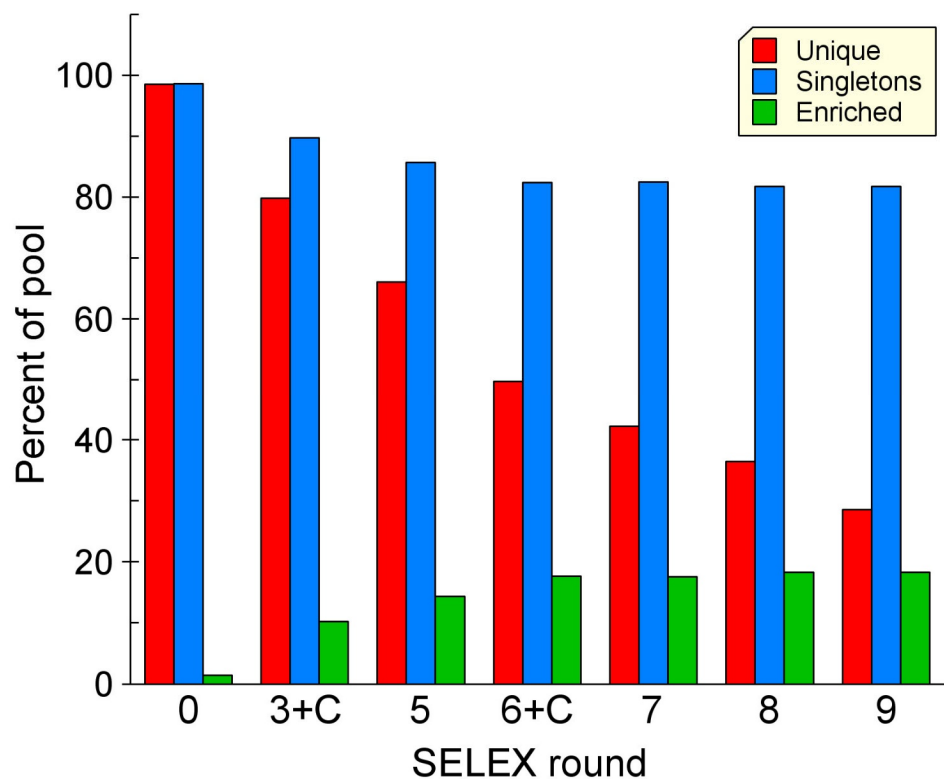
Legend: All siderophores (PWD-Pf5, ENB and ORB) were in the ferric form. PVD-Pf5 (pyoverdine Pf5), ENB (enterobactin) and ORB (ornibactin).

Supplementary materials

4 Supplementary Figures

4.1 Figure S1

Analysis of NextGen sequencing results

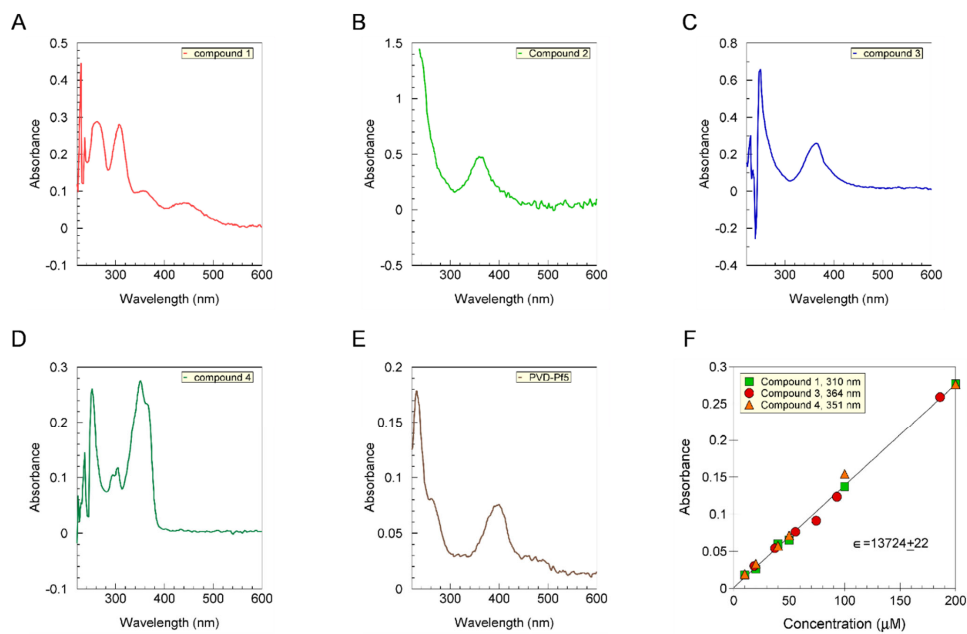


LEGEND: The percent of each round identified as the unique fraction (number of species in pool divided by pool size), Singletons (species present only once in the database) and Enriched species (species present more than once in the database) is plotted for the original pool (round 0) and rounds 3 through 9. Rounds 3 and 6 include counterselections that were performed after the identified selection round.

Supplementary materials

4.2 Figure S2

uv/vis absorption spectra of synthesized compounds 1-4

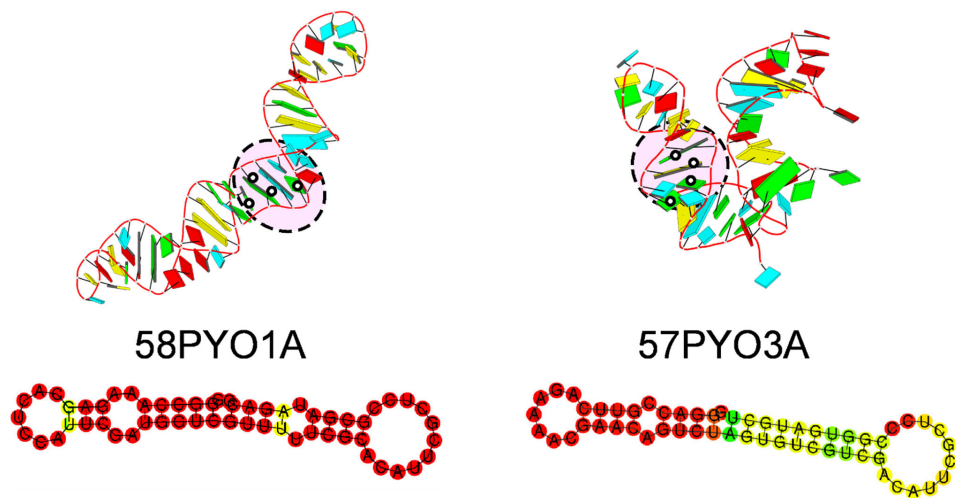


LEGEND: A-E UV-Vis spectra of compound 1, 2, 3, 4 dissolved in DMSO and PVD-Pf5 dissolved in water, F) Concentration vs absorbance at maximum (310nm, 359nm, 364nm, 351nm, and 400nm for 1, 2, 3, 4 and PVD-Pf5 respectively) to determine the extinction coefficients of compounds 1, 3 and 4.

Supplementary materials

4.3 Figure S3

Predicted structures

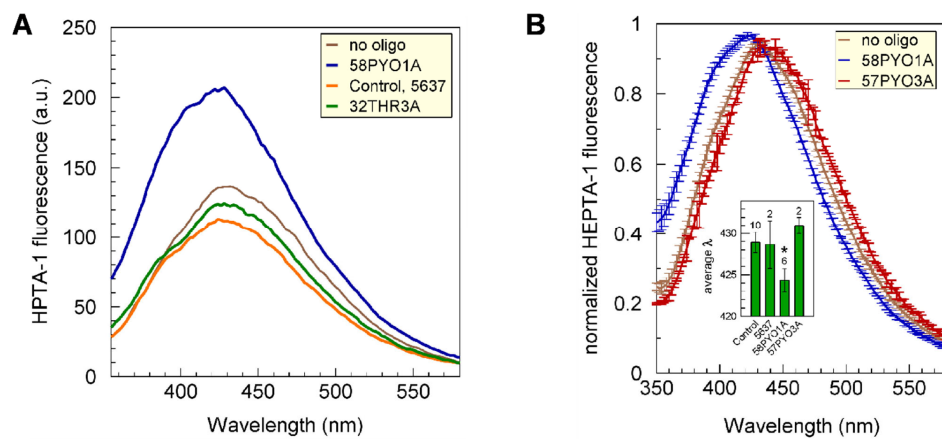


LEGEND: **Top:** 3D structures of 58PYO1A and 57PYO3A predicted using 3dRNA and visualized using x3DNA. The black circles identify the positions of Gs proposed to form a G-quartet. **Bottom:** 2D structural renditions predicted by RNA fold.

Supplementary materials

4.4 Figure S4

The effect of aptamers on the fluorescence spectrum of HPTA-1

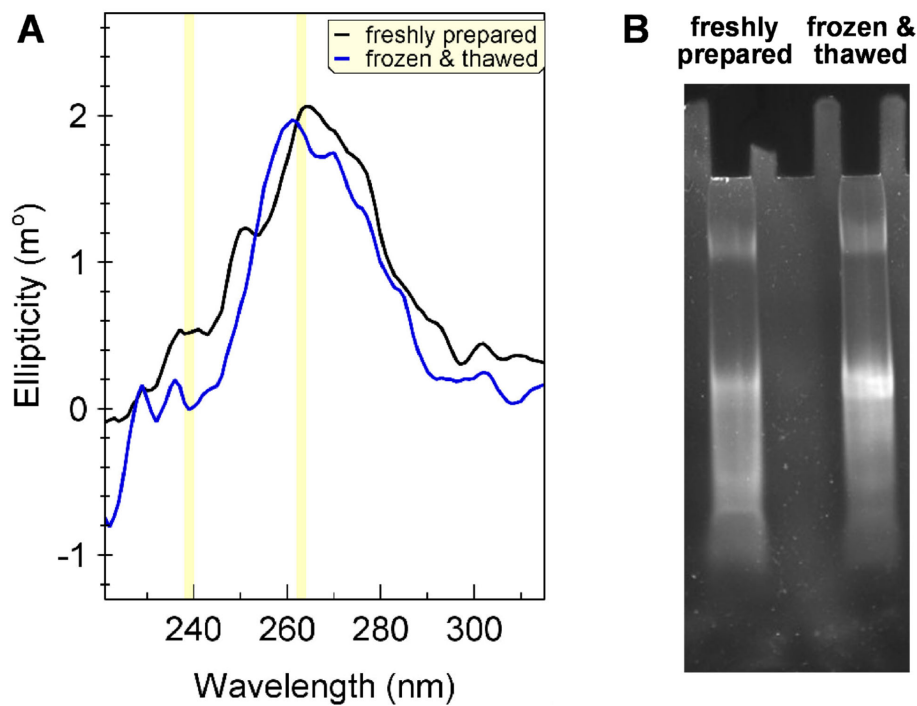


LEGEND: A. The fluorescence of spectra ($\lambda^{\text{ex}} = 304$ nm and λ^{em} scan (350-600 nm) of 6 μM HPTA-1 alone and in combination with the 2 μM identified oligonucleotides are plotted with from 340-590 nm. Single smoothed spectra are shown. **B.** The fluorescence of spectra ($\lambda^{\text{ex}} = 304$ nm and λ^{em} scan (350-600 nm) of 6 μM HPTA-1 alone and in combination with the 2 μM 58PYO1A or 57PYO3A. Individual spectra were first normalized to the maximum peak height for each spectrum then independently obtained normalized spectra were averaged for each condition and the averaged spectra smoothed. Contributing numbers of independent spectra were “no oligonucleotide” (10), 58PYO1A (6) and 57PYO3A (2). The SEM for the spectral averages are shown.

Supplementary materials

4.5 Figure S5

The effect of freeze-thaw on the CD spectrum and molecular size of 57PYO3A

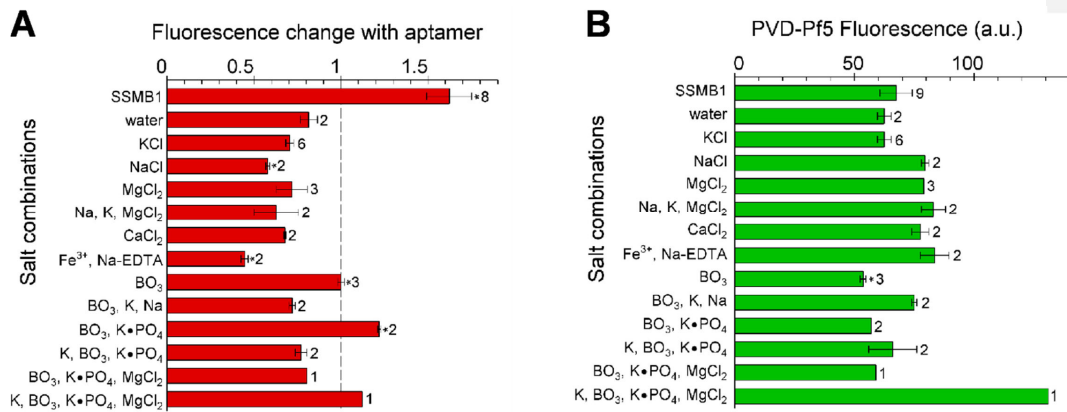


LEGEND: **A.** CD spectra 2uM of 57PYO3A for freshly prepared and frozen thawed (-20 °C for 18 h then to 23 °C) sample in SSMB1. Each spectrum is the smoothed average of two independent CD spectral collections of 3 scans each. **B.** nondenaturing gel electrophoresis of 57PYO3A when freshly prepared and after freeze-thaw.

Supplementary materials

4.6 Figure S6

The effect of salt combinations on PVD-Pf5 binding to 57PYO3A

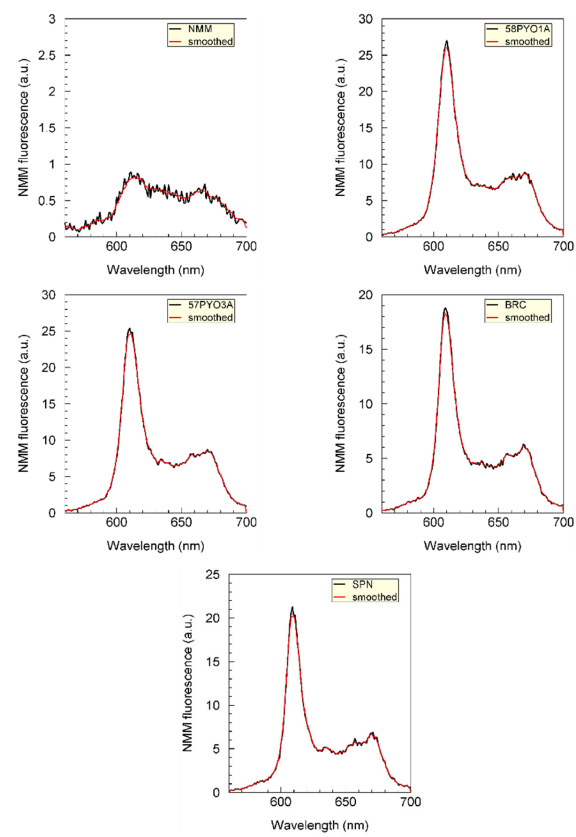


LEGEND: **A.** For each salt combination, the maximum PVD-Pf5 fluorescence (measured at 460–466 nm, depending on the spectrum) in the presence of 400 nM aptamer was divided by the maximum fluorescence in its absence. The mean ratio from all experiments for each salt mix is shown as red bars, with error bars indicating the standard error of the mean. **B.** The fluorescence of PVD-Pf5 in the absence of aptamer is shown for each salt mixture in A. Statistical significance relative to water alone was assessed using the Student's *t*-test ($p < 0.05$). Numbers to the right of the bars indicate the number of independent measurements used to calculate each mean. Phosphate was supplied as KH₂PO₄, abbreviated here as K•PO₄.

Supplementary materials

4.7 Figure S7

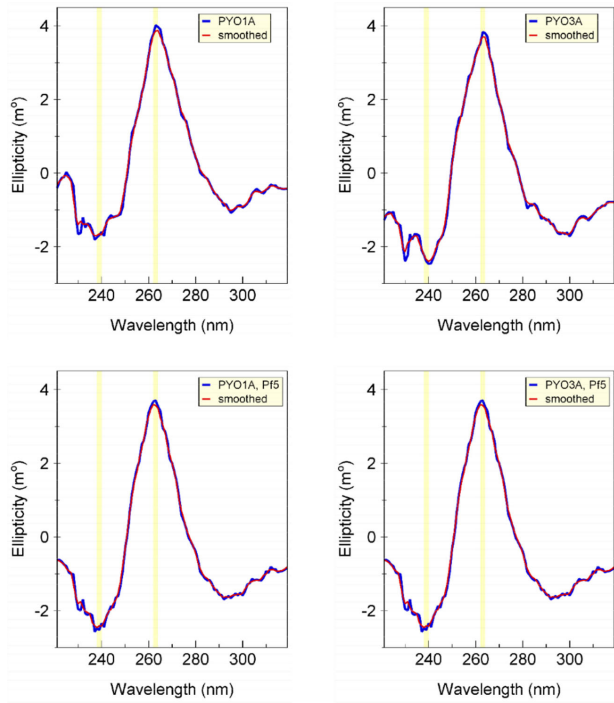
Raw data for NMM spectra in Fig. 4D with and without smoothing



Supplementary materials

4.8 Figure S8

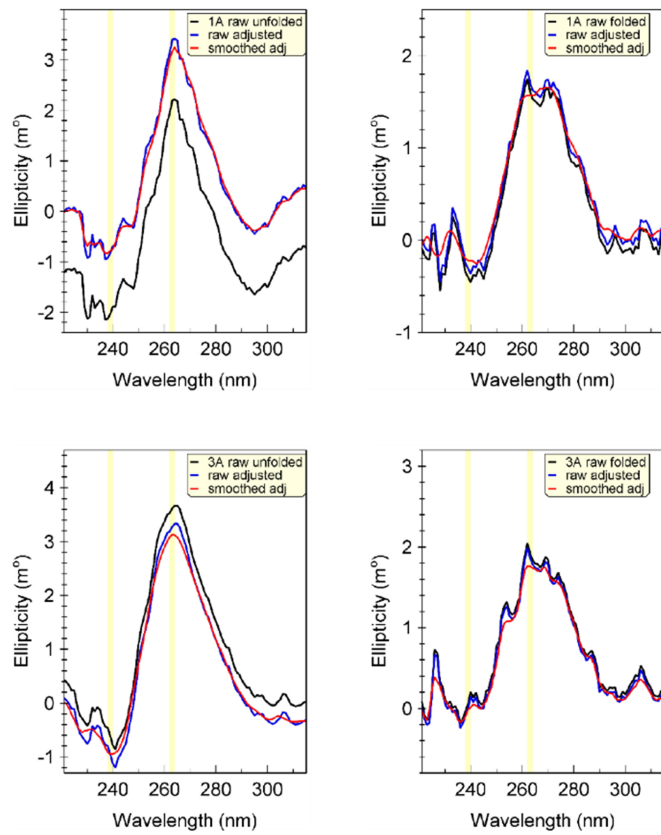
Raw data for CD spectra in Fig. 4E with and without smoothing



Supplementary materials

4.9 Figure S9

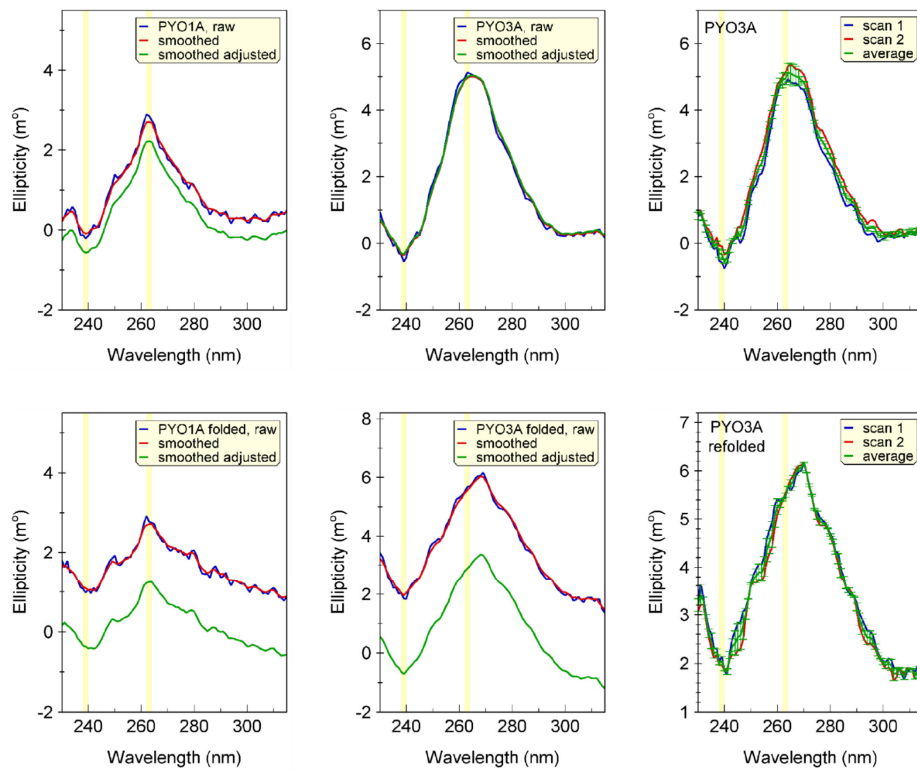
Raw data for CD spectra in Fig. 5B with and without baseline adjustments and smoothing



Supplementary materials

4.10 Figure S10

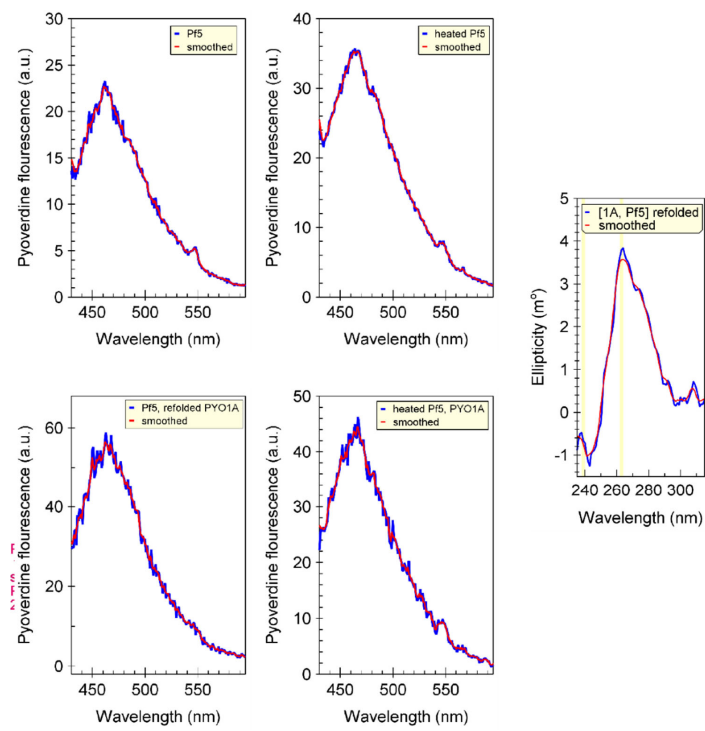
Raw data for CD spectra in Fig. 5C with and without baseline adjustments and smoothing



Supplementary materials

4.11 Figure S11

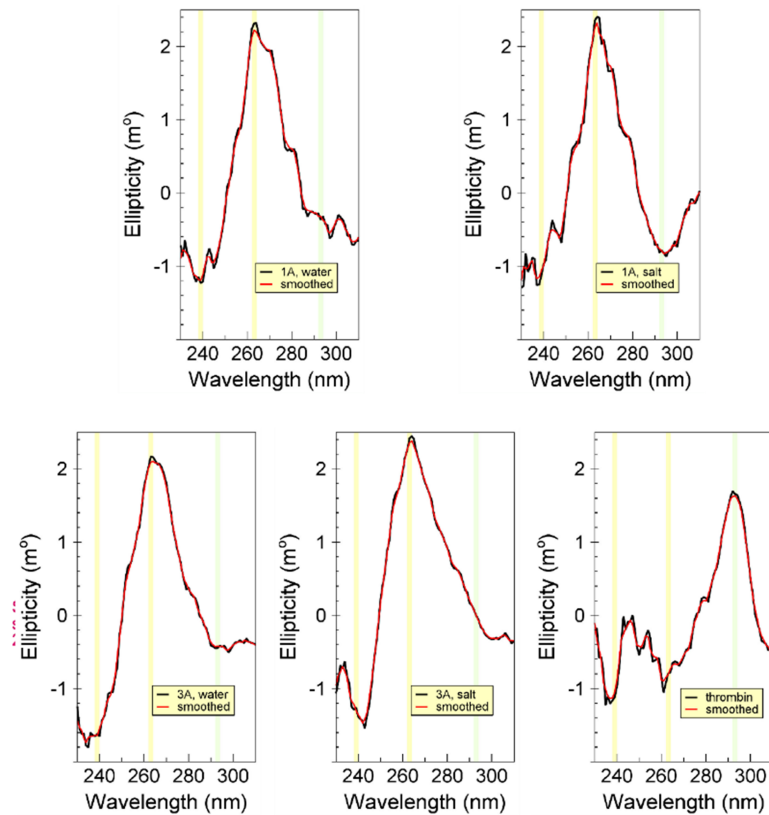
Raw data for CD spectra in Fig. 5C with and without baseline adjustments and smoothing



Supplementary materials

4.12 Figure S12

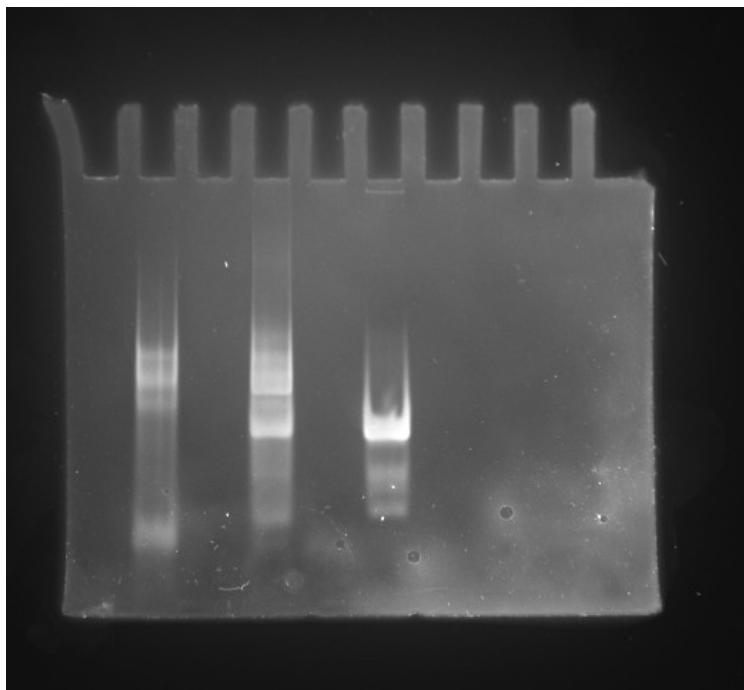
Raw data for CD spectra in Fig. 6C with and without smoothing



Supplementary materials

Figure S13

Full gel image for Figure 4G



5 Citations

1. Levine, H.A., and Nilsen-Hamilton, M. A mathematical analysis of SELEX. *Comput Biol Chem* **31**, 11-35 10.1016/j.combiolchem.2006.10.002 (2007).
2. Hoinka, J., Backofen, R., and Przytycka, T.M. Aptasuite: A Full-Featured Bioinformatics Framework for the Comprehensive Analysis of Aptamers from HT-SELEX Experiments. *Molecular therapy. Nucleic acids* **11**, 515-517 10.1016/j.omtn.2018.04.006 (2018).